ACS APPLIED MATERIALS & INTERFACES

Research Article

www.acsami.org

Clay–Chitosan Nanobrick Walls: Completely Renewable Gas Barrier and Flame-Retardant Nanocoatings

Galina Laufer, Christopher Kirkland, Amanda A. Cain, and Jaime C. Grunlan*

Department of Mechanical Engineering, Texas A&M University, College Station, Texas 77843, United States

Supporting Information

ABSTRACT: Thin films prepared via a layer-by-layer (LbL) assembly of renewable materials exhibit exceptional oxygen barrier and flame-retardant properties. Positively charged chitosan (CH), at two different pH levels (pH 3 and pH 6), was paired with anionic montmorillonite (MMT) clay nanoplatelets. Thin-film assemblies prepared with CH at high pH are thicker, because if the low polymer charge density. A 30-bilayer (CH pH 6-MMT) nanocoating (~100 nm thick) reduces the oxygen permeability of a 0.5-mm-thick polylactic acid film by four orders of magnitude. This same coating system completely stops the melting of a flexible polyurethane foam, when exposed to direct flame from a butane torch, with just 10 bilayers (~30 nm thick). Cone calorimetry confirms that this coated foam exhibited a reduced peak heat-release rate, by as much as 52%, relative to the uncoated control. These environmentally benign nanocoatings could prove beneficial for new types of food packaging or a replacement for environmentally persistent antiflammable compounds.

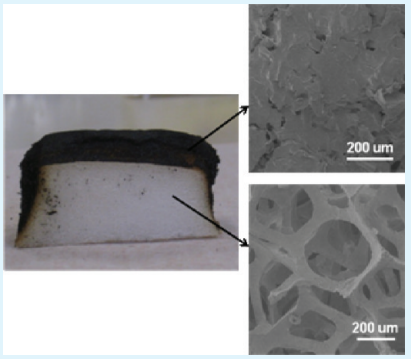

KEYWORDS: *layer-by-layer assembly, polyurethane foam, oxygen permeability, heat release rate, flame (or fire) retardant (or resistant)*

Polysaccharides are naturally occurring polymers that are widely available in nature. Of the many types of polysaccharides, chitin is the second most abundant after cellulose.[1] Chitin is extracted from the shells of crustaceans (e.g., lobsters and shrimp) and the exoskeletons of arthropods (e.g., insects). Despite its abundance, unmodified chitin's usefulness is very limited, because of its poor solubility in most solvents. Chitosan, which is an amino polysaccharide obtained via the alkaline deacetylation of chitin (see the structure in Figure 1),[2] is soluble in acidic aqueous solutions, because of the protonation of its amino groups at pH <6.2.[3,4] In addition to its solubility, chitosan is biodegradable, biocompatible, and benign. These traits have led to the significant study of chitosan's use in biomedical applications, such as drug delivery,[5−8] wound-dressing materials,[9−11] artificial skin,[12−14] and blood anticoagulants.[15,16] Chitosan's positive charge at low pH also allows it to be alternately deposited with negatively charged molecules or nanoparticles to produce multilayer thin films from aqueous solutions.[1,17]

Layer-by-layer (LbL) assembly is a technique that allows the construction of multilayered films through the alternate deposition of oppositely charged polyelectrolytes or particles on a substrate.[18−20] Surface charge inversion during each adsorption step limits the thickness of each layer and prepares the surface for the subsequent adsorption of the oppositely charged polyelectrolyte. Each positive and negative pair deposited is referred as a bilayer (BL). The thickness of a single bilayer is typically 1−100 nm, and the LbL method allows for significant tailoring on the nanoscale level.[21−23] This technique has been used to grow multilayered films with various properties, including water repellant,[24,25] controlled drug release,[26,27] oxygen barrier,[28,29] chemical sensing,[30−32] antimicrobial,[33−35] and flame retardant.[36−38]

In several instances, a polymer has been paired with clay nanoplatelets to improve the mechanical,[39,40] thermal,[41,42] and barrier[43−45] properties of the substrate. Montmorillonite (MMT) is the most widely used anionic clay and is part of the smectite group. The MMT structure consists of two fused tetrahedral layers of silica sandwiching an octahedral layer of alumina and magnesia (as shown in Figure 1).[46] In addition to being exfoliated in water to produce 1-nm-thick anionic platelets ($l/d \approx 200$), montmorillonite is benign, naturally abundant, and relatively low cost.

In an effort to create fully renewable and multifunctional assemblies, thin films of chitosan and MMT clay were deposited on polyurethane (PU) foam and polylactic acid (PLA) film. PU and PLA were tested, respectively, for flame-retardant and oxygen-barrier properties. These polymer−clay thin films resemble nanobrick walls, with CH acting as the mortar holding the MMT bricks together. In terms of fire safety, PU foam (without flame-retardant additives) is very flammable, often resulting in the dripping of melted material, which enhances flame spread through the formation of a pool fire under the burning object. If the pool fire is close enough to another flammable object, the result can be a self-propagating fire.[47] Just 10 bilayers of CH pH 6-MMT cuts the peak heat-release rate of open-celled, flexible PU foam in half. This same treated foam maintains its shape, with no signs of melting,

Received: December 17, 2011
Accepted: February 16, 2012
Published: February 16, 2012

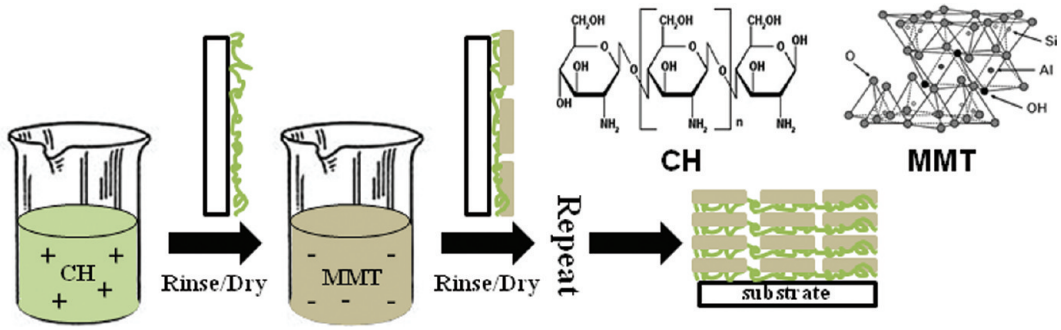

Figure 1. Schematic representation of layer-by-layer (LbL) assembly with chitosan (CH) and montmorillonite clay (MMT). This process is repeated until the desired number of bilayers is deposited.

when exposed to direct flame from a butane torch for 10 s. Oxygen-barrier properties were tested on a PLA film, which can be produced from renewable resources such as starch.[48] PLA is a high-strength thermoplastic polymer that is biodegradable and compostable.[49] However, it has poor oxygen-barrier properties, relative to the petroleum-based polymers that are widely used as food packaging (e.g., poly(ethylene terephthalate)).[50] A 70-nm CH pH 6-MMT assembly (i.e., 20 BL) reduces the oxygen transmission rate (OTR) of a 0.5-mm-thick PLA film by two orders of magnitude. These results demonstrate the ability to create a fully renewable nanocoating capable of imparting a gas barrier to plastic film (e.g., for food packaging) and significant fire resistance to PU foam (e.g., for building insulation or furniture padding).

RESULTS AND DISCUSSION

Film Growth and Microstructure. Growth of chitosan–clay assemblies, as a function of the number of bilayers deposited (Figure 2a), was monitored using ellipsometry. Both films exhibit linear growth, but the film growth at pH 6 is much thicker than the growth at pH 3. It was previously shown that LbL deposition results in the majority of clay platelets being deposited as a single layer,[43] which means that the difference in thickness is primarily influenced by chitosan deposition. Chitosan has primary amine groups that make its conformation and charge density pH-dependent, which influences the thickness of adsorbed layers. At pH 3, chitosan is fully ionized and electrostatic repulsions of the free ammonium groups cause the polymer chains to become elongated and deposit very thinly onto a substrate.[51] As the polymer pH increases, the amines become deprotonated and ionic repulsions are reduced, leading to a more globular conformation of the chains. Lack of self-repulsion leads to thicker films, as shown in Figure 2a. These same trends are observed when growth is measured as a function of weight deposited, using a quartz crystal microbalance (QCM).

Figure 2b shows the weight of each deposited layer for films made with the pH 3 or pH 6 chitosan. The growth trend of both systems is similar to the linear trend observed with ellipsometry (Figure 2a), with higher pH generating heavier layers. It is interesting to note that films at pH 6 also have higher clay loading (expressed in terms of weight percent in Table 1), which is somewhat counterintuitive. Previous work with clay–polyethylenimine assemblies showed that thicker polymer deposition resulted in lower clay concentration, because of greater spacing between single clay layers.[43] High-pH (low-charge-density) chitosan deposits less uniformly, creating a rough surface (see the AFM image in Figure S1 in the Supporting Information). This nanoscopic roughness provides greater surface area for clay platelets to deposit onto (see the proposed schematic of this structure in Figure 2a). At low pH, the polymer deposits smoothly onto a substrate and clay can only deposit parallel to the substrate. The higher clay concentration at pH 6 results in a higher density of the films (Table 1).

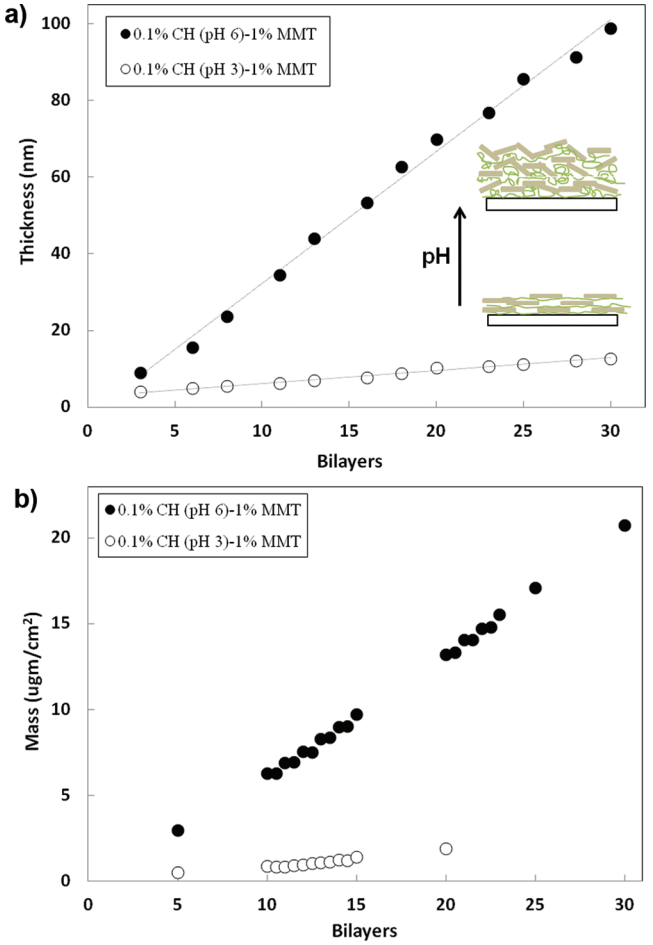

Figure 2. (a) Thickness and (b) mass of chitosan–clay assemblies, as a function of the number of bilayers deposited.

Table 1. Composition and Density of CH-MMT Assemblies[a]

	CH (wt %)	MMT (wt %)	density (g/cm³)
CH pH 3-MMT	33.79	66.21	1.19
CH pH 6-MMT	10.69	89.31	1.89

[a]See the Supporting Information for calculations.

Transmission electron microscopy (TEM) cross sections of 100 BL films made with pH 3 and pH 6 chitosan (CH pH 3 and CH pH 6, respectively) are shown in Figure 3. These

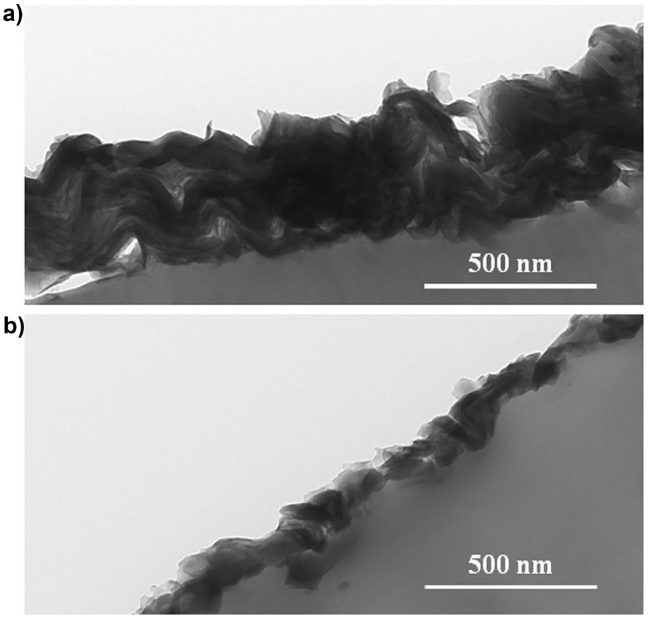

Figure 3. TEM cross sections of (a) 100-BL CH pH 6-MMT and (b) 100-BL CH pH 3-MMT deposited on polystyrene.

images clearly show the high level of clay orientation and the structural differences between high and low pH (resembling the schematic images in Figure 2a) The film deposited with CH pH 6 (Figure 3a) is much thicker than that made with CH pH 3 (Figure 3b) and also shows some misaligned clay platelets. Furthermore, the thickness of these films agrees well with the value extrapolated from the ellipsometric growth curves in Figure 2a. This nanobrick wall structure has already been shown to exhibit low oxygen permeability and flame-retardant behavior.[28,36]

Oxygen Barrier on Polylactic Acid. Polylactic acid (PLA) has received significant attention recently, because of a desire for biodegradable food packaging.[52] It has already been approved for food contact by the Food and Drug Administration (FDA) and has been primarily used for the packaging of short shelf life food, because of the poor oxygen-barrier properties.[53,54] Improving the oxygen barrier of PLA film will allow it to slow oxidative degradation and increase food shelf life.[55] It was previously shown that increasing the space between deposited clay layers significantly improves the oxygen barrier of nanobrick wall films,[43] so CH pH 6-MMTbilayers were deposited onto PLA for this purpose. Table 2 shows how the oxygen transmission rate (OTR) of these films decreases with the number of bilayers deposited. With just 10 BL, there is an order-of-magnitude decrease in OTR relative to the same PLA film with no coating. A 30 BL film, which is only 100 nm thick, exhibits an OTR below the detection limit of commercial instrumentation ($\leq$0.005 $cm^3/(m^2$ day atm)). This high-barrier behavior is believed to be due to the brick wall nanostructure, which produces an extremely tortuous path for oxygen molecules to take as they permeate through the film.[56,57]

Even though chitosan is known to have an intrinsically low oxygen barrier,[59,60] its permeability is orders-of-magnitude-higher than that of typical packaging films, as summarized in Table 3. The addition of clay directly to PLA or chitosan-based films provides

Table 2. Oxygen Permeability of CH pH 6-MMT Assemblies on PLA Film at 23 °C

number of BL	film thickness (nm)	OTR ($cm^3/(m^2$ atm day))	Permeability ($\times 10^{-16}$ cm^3 cm/(cm^2 s Pa)) film[ab]	Permeability ($\times 10^{-16}$ cm^3 cm/(cm^2 s Pa)) total[b]
0	N/A	30.54	N/A	177.2
10	31.8	2.51	0.0019	14.6
15	48.9	0.68	0.0008	4.0
20	69.8	0.44	0.0006	2.6
25	85.6	0.13	0.0002	0.8
30	98.7	<0.005	<0.000008	<0.03

[a]Film permeability was decoupled from the total permeability using a previously described method.[58] [b]The low-end detection limit for an Ox Tran 2/21 L module is 0.005 $cm^3/(m^2$ day atm).

Table 3. Oxygen Permeability of Various Barrier Materials

film composition	permeability ($\times 10^{-16}$ cm^3 cm/(cm^2 s Pa))[a]	reference
pure chitosan	1770000	61
chitosan/10 wt % clay	141000	61
PLA/10 wt % clay	50.49	62
PET	17.3	29
EVOH	0.0571	63
30 BL CH/MMT on PLA film	<0.03	Table 2

[a]All measurement were performed at 23 °C and 0% RH.

only a moderate reduction in oxygen permeability. In conventional thick film (i.e., bulk) composites, there is a loading limit for inorganic filler (~10 wt %), beyond which the composite mechanical properties and transparency degrade, while LbL assembly provides the ability to create composites with 90 wt % clay. As a result, PLA film coated with 10 BL of CH-MMT has permeability equivalent to that of bare PET film (see Table 3), which is considered to be a good barrier to oxygen. In addition to having outstanding barrier properties, this nanocoating can impart antiflammable characteristics to foam.

Flame-Retardant Behavior on Polyurethane Foam. Ten bilayers of high- and low-pH chitosan and clay were deposited onto open-celled, flexible polyurethane (PU) foam. The weight added to foam was determined by weighing before and after coating (reported as a percentage of the original mass in Table 3). Figure 4 shows the surfaces of an uncoated control and foam coated with CH pH 3-MMT and CH pH 6-MMT (see Figures 4a, 4b, and 4c, respectively). The control foam is very smooth, while the coated foam has a uniform nanotexture that confirms the conformal nature of LbL deposition. The images in Figure 4 are representative images of how the foam looks throughout its entire thickness, revealing excellent coverage of every pore wall without altering the macroscale porosity of the foam. As expected, the pH 6 coating (Figure 4b) appears heavier (i.e., has a stronger texture) than the thinner (<10 nm) pH 3 coating (Figure 4c).

Foam flammability was initially tested by holding the flame from a butane torch on the foam's surface for 10 s. The uncoated foam ignited and started to melt immediately upon exposure to the flame and was ultimately destroyed (i.e., completely consumed). No melt dripping was exhibited by either of the coated foam samples, and the flame was extinguished after it traveled across the foam surface (~30 s). Foam coated with 10 BL of CH pH 6-MMT retained its original shape after flame exposure (Figure 5a), while foam coated with CH pH 3-MMT slightly collapsed (Figure 5b). When cut

dx.doi.org/10.1021/am2017915 | ACS Appl. Mater. Interfaces 2012, 4, 1643–1649

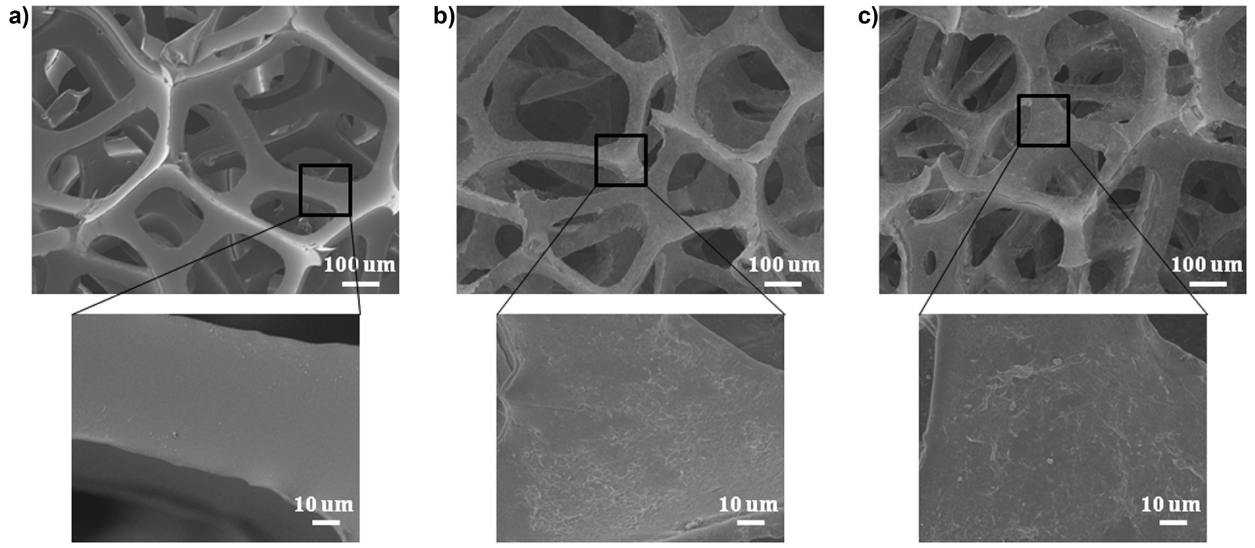

Figure 4. Scanning electron microscopy (SEM) images of (a) uncoated polyurethane foam and (b,c) foam coated with 10 BL of CH pH 3-MMT (panel b) and CH pH 6-MMT (panel c).

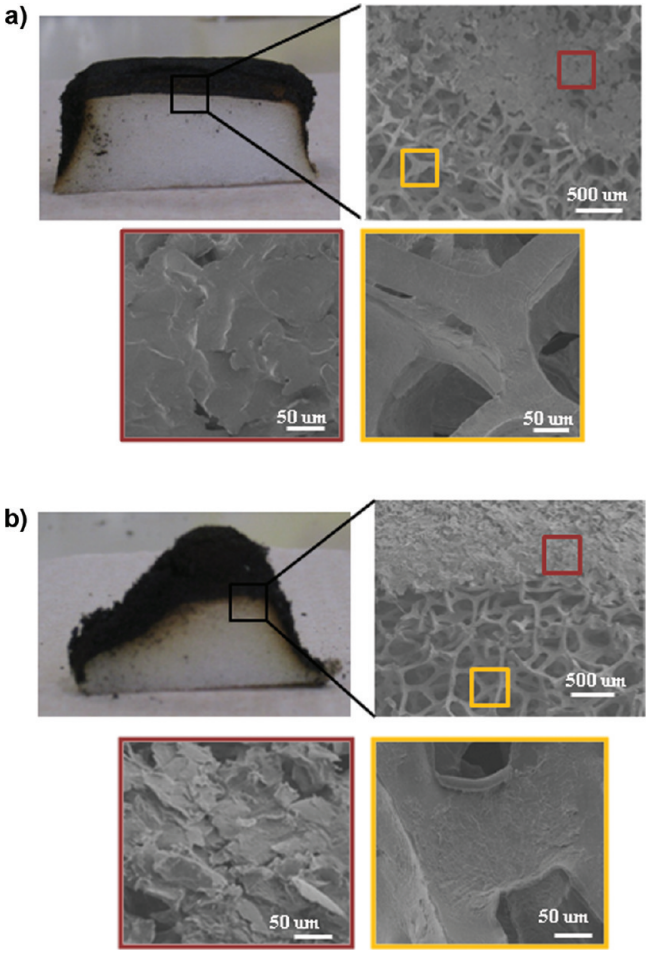

Figure 5. SEM images of cross sections of foam coated with 10 BL of (a) CH pH 6-MMT and (b) CH pH 3-MMT following the torch burn test. Boxes of the same color correlate to spots that were further magnified in each foam.

through the middle, coated foam samples revealed flexible, undamaged (white) foam underneath the char. Higher-magnification images of the interface between the black char and white foam reveal that the foam structure was not damaged and the char consists mostly of aggregated clay platelets. Coating with pH 6 chitosan (Figure 5a) provides a more protective barrier, because of its greater thickness and higher clay content than the pH 3 chitosan.

In an effort to better understand the effect of the CH-MMT coating on the flammability of PU foam, cone calorimetry was performed on these 10-BL-coated samples. A cone calorimeter quantitatively measures the inherent flammability of a material through the use of oxygen consumption calorimetry (ASTM E-1354/ISO 5660). Figure 6 shows the heat-release rate (HRR)

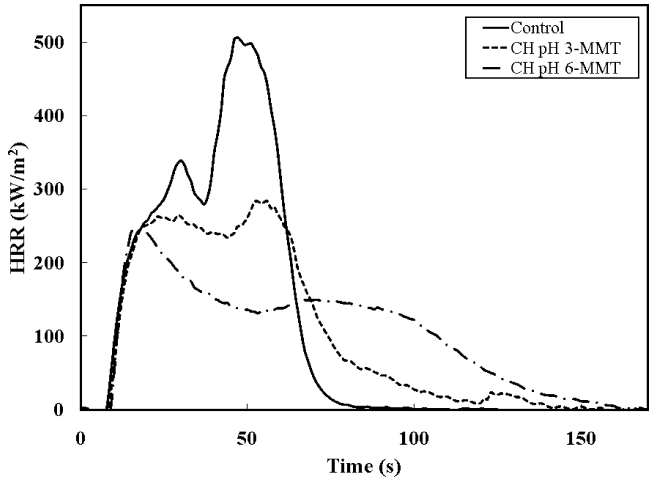

Figure 6. Heat-release rate (HRR), as a function of time, during cone calorimeter testing, for uncoated control and 10-BL-coated foam.

curves for control and coated foam samples. Two different peaks can be seen in the curve for the control foam. There is a rapid rise to the first peak soon after ignition, which is associated with foam collapse. After its transformation to a liquid, PU burning tends to accelerate as the decomposing material vaporizes quickly, which quickly leads to a fast progression to a second, larger-peak HRR. The decay after the peak is also very rapid, with all material being decomposed.[64] HRR curves for coated foam samples are significantly different

dx.doi.org/10.1021/am2017915 | ACS Appl. Mater. Interfaces 2012, 4, 1643–1649

Table 4. Cone Calorimeter Results for the Control and the 10-BL-Coated Foam[a]

sample	weight gain (%)	pkHRR (kW/m^2)	avg HRR (kW/m^2)	total HRR (mJ/m^2)	mass loss (%)	MAHRE (kW/m^2)
control		517 ± 33.9	178 ± 12.5	18.9 ± 1.6	100	286 ± 22.6
CH pH 3-MMT	1.59	326 ± 60.9	144 ± 18.6	17 ± 0.2	94 ± 1.8	209 ± 46.2
CH pH 6-MMT	4.01	246 ± 5.4	116 ± 7.9	17 ± 0.4	93 ± 1.4	148 ± 7.7

[a]HRR = heat-release rate; pkHRR = peak heat-release rate; MAHRE = maximum average heat rate emission.

from the control, suggesting that the CH-MMT coating fundamentally changes the burning behavior of the foam.

Ten bilayers of CH pH 6-MMT, which is ∼30 nm thick, completely eliminates the second HRR peak. This coating produced the largest reduction (52%) in peak heat-release rate (pkHRR), which is the maximum value of the heat-release rate during the combustion of the sample. It also reduced the average heat-release rate (Avg HRR) by more than 30% and maximum average heat rate emission (MAHRE) by almost 50%. MAHRE is an ignition modified rate of heat emission, which can be used to rank materials in terms of ability to support flame spread to other objects.[65] CH pH 3-MMT also reduced these flammability values, but not as dramatically as CH pH 6-MMT. This was expected , because of the higher clay concentration in the pH 6 coating, which was able to form a thicker, more effective protective layer. Furthermore, the pyrolysis of PU decomposition products was delayed, because these foams never collapsed into a liquid. Longer burning times for coated foam ultimately caused the total heat release to be similar to the control, but these CH-MMT coatings make a dramatic difference in the reduction of flammability of foam. The cone calorimeter parameters are summarized in Table 4. When comparing the pkHRR reduction to clay-filled polymers in the literature, the 10 BL CH-MMT nanocoating achieves a reduction similar to the best performing materials, as shown in Table 5.

Table 5. Cone Calorimeter Values Reported in Literature for Clay Composites

sample	pkHRR reduction (%)	reference
polyethylene/2-15% clay	50−70	66
polystyrene/1-10 % clay	8−23	67
polypropylene/5% clay	33	68
polyamide 6/15% clay	60	69
PU/10 BL CH pH 6-MMT polyurethane foam	52	Table 4

CONCLUSIONS

The goal of this work was to develop a truly "green" film with flame-retardant and oxygen-barrier characteristics. Films assembled with high-pH or low-pH chitosan (CH) and clay (montmorillonite, MMT) showed linear growth as a function of the number of bilayers deposited. Higher chitosan pH resulted in much thicker assemblies with higher clay loading. An oxygen permeability of $<0.03 \times 10^{-16}$ cm^3 cm/(cm^2 s Pa) was achieved with 30 bilayers (30 BL) of CH pH 6-MMT (< 100 nm thick). The combination of all of these features—it is generally recognized as a safe material, it has high oxygen barriers, and the transparency exhibited by this film—makes it an ideal candidate for food and other types of high-performance packaging. When a flexible polyurethane (PU) foam was coated with 10 BL of CH pH 6-MMT, only the outermost surface was charred after being exposed to the direct flame from a propane torch for 10 s. When cut open, an undamaged white flexible foam was revealed under a black char layer. Cone calorimetry revealed that this protective nanocoating significantly reduced the peak heat release, relative to the uncoated control, showing a maximum reduction of 52%. This work demonstrates the first fully renewable flame-retardant treatment made via layer-by-layer (LbL) assembly and provides an environmentally benign alternative to commonly used halogenated materials.

EXPERIMENTAL SECTION

Materials. Cationic deposition solutions were prepared by adjusting the pH of deionized water (18.2 MΩ, pH ∼5.5) to 2 with hydrochloric acid (HCl) and then adding 0.1 wt % chitosan (MW 50−190 kDa, 75%−85% deacetylated) purchased from Aldrich (Milwaukee, WI). This aqueous solution was magnetically stirred for 24 h until the chitosan was completely dissolved. The solution pH was adjusted to 3 or 6 with 1 M NaOH just prior to deposition. Anionic solutions were prepared by adding 1.0 wt % of sodium montmorillonite (trade name: Cloisite Na$^+$), provided by Southern Clay Products, Inc. (Gonzales, TX), to deionized water and rolling the material for 24 h. This MMT has a cationic exchange capacity of 0.926 mequiv/g and a negative surface charge in deionized water.[70] Individual platelets have a density of 2.86 g/cm^3, with a planar dimension of 10−1000 nm (average is ∼200 nm) and a thickness of 1 nm.[71] Single-side-polished (1 0 0) silicon wafers (University Wafer, South Boston, MA) were used as the substrate for film thickness characterization and 125-μm-thick polystyrene (PS) film (Goodfellow, Oakdale, PA) was used for TEM images. Polylactic acid (PLA) films, with a thickness of 500 μm, were used for oxygen-barrier testing. Polyester-based polyurethane (PU) foam (United Foam, Denver, CO), with 100 pores per linear inch (ppi) and without flame-retardant additives, was used for the flammability experiments.

Layer-by-Layer (LbL) Deposition. Prior to deposition, the silicon wafers were rinsed with acetone and deionized water, and then dried with filtered air. In the case of PS and PLA, methanol was used in place of acetone. These substrates were then corona-treated, using a Model BD-20C Corona Treater (Electro-Technic Products, Inc., Chicago, IL), to create a negative surface charge. Foam samples were dipped into 0.1 M nitric acid for 30 s prior to LbL deposition, and then dipped into a 1 wt % branched polyethylenimine solution (pH 10, molecular weight of MW = 25 kDa) as a primer layer, to improve adhesion. All films were deposited on a given substrate, using the procedure shown schematically in Figure 1. Substrates were alternately dipped into positive and negative mixtures. Initial dips were 5 min each, and subsequent dips were 1 min. Each dip was followed by rinsing with deionized water and, in the case of the silicon wafer, PS, or PLA film, drying with air. Foams were wringed out to expel liquid as an alternative to the traditional drying step. After the desired number of bilayers was deposited, foam samples were dried at 80 °C in an oven for 2 h before testing.

Characterization of Film Growth, Structure, and Properties. Film thickness was measured with a Model alpha-SE Ellipsometer (J.A. Woollam Co., Inc., Lincoln, NE). The weight per deposited layer was measured with a Maxtek Research Quartz Crystal Microbalance (RQCM) (Infinicon, East Syracuse, NY), with a frequency range of 3.8−6 MHz, in conjunction with 5 MHz quartz crystals. Cross sections of clay−chitosan assemblies were imaged via transmission electron microscopy (TEM; Model 1200 EX, JEOL, Ltd., Tokyo, Japan), operated at 110 kV. Samples were prepared for imaging by embedding a piece of PS supporting the LbL film in epoxy and sectioning it with a microtome equipped with a diamond knife. Surface images of the control and coated foam samples were acquired via field-emission scanning electron microscopy (FESEM; Model JSM-7500F, JEOL, Ltd., Tokyo, Japan). Platinum coating of 8 nm was deposited on all samples prior to the imaging, to prevent charging. The surface topography was imaged via atomic force microscopy (AFM; Nanosurf EasyScan 2 system, Nanoscience Instruments, Inc., Phoenix, AZ). Foam flammability was evaluated by exposure to direct flame from a butane micro torch (Model ST2200, Benzomatic, Huntersville, NC) for 10 s (the approximate flame temperature is 2400 °F, blue flame). Cone calorimetry was performed at the University of Dayton Research Institute, using an FTT Dual Cone Calorimeter at one heat flux (35 kW/m^2), with an exhaust flow of 24 L/s, using the standardized cone calorimeter procedure (ASTM E-1354-07). Oxygen transmission rate of thin films on PLA was measured by MOCON (Minneapolis, MN) in accordance with ASTM D-3985, using an Oxtran Model 2/21 ML instrument at 23 °C and 0% relative humidity (RH).

■ ASSOCIATED CONTENT

Ⓢ Supporting Information

AFM topography scans of a single chitosan layer at pH 3 and pH 6. This material is available free of charge via the Internet at http://pubs.acs.org.

■ AUTHOR INFORMATION

Corresponding Author

*Tel.: +1 979 845 3027. Fax: +1 979 862 3989. E-mail address: jgrunlan@tamu.edu.

Notes

The authors declare no competing financial interest.

■ ACKNOWLEDGMENTS

The NIST Building and Fire Research Lab is gratefully acknowledged for financial support of this work.

■ REFERENCES

(1) Lee, D. W.; Lim, H.; Chong, H. N.; Shim, W. S. *Open Biomed. J.* **2009**, *1*, 10−20.
(2) El-Tahlawy, K.; Hudson, S. M. *J. Appl. Polym. Sci.* **2006**, *100*, 1162−1168.
(3) Kurita, K. *Prog. Polym. Sci.* **2001**, *26*, 1921−1971.
(4) Desbrieres, J. *Polymer* **2004**, *45*, 3285−3295.
(5) Prabaharan, M. *J. Biomater. Appl.* **2008**, *23*, 5−36.
(6) Shu, X. Z.; Zhu, K. J. *Int. J. Pharm.* **2002**, *233*, 217−225.
(7) Felt, O.; Buri, P.; Gurny, R. *Drug Dev. Ind. Pharm.* **1998**, *24*, 979−993.
(8) Lee, K. Y.; Kwon, I. C.; Kim, Y.-H.; Jo, W. H.; Jeong, S. Y. *J. Controlled Release* **1998**, *51*, 213−220.
(9) Mi, F.-L.; Shyu, S.-S.; Wu, Y.-B.; Lee, S.-T.; Shyong, J.-Y.; Huang, R.-N. *Biomaterials* **2001**, *22*, 165−173.
(10) Kim, H. J.; Lee, H. C.; J.S., O.; Shin, B. A.; Oh, C. S.; Park, R. D.; Yang, K. S.; Cho, C. S. *J. Biomater. Sci., Polym. Ed.* **1999**, *10*, 543−556.
(11) Mi, F.-L.; Wu, Y.-B.; Shyu, S.-S.; Schoung, J.-Y.; Huang, Y.-B.; Hao, J.-Y. *J. Biomed. Mater. Res., Part B* **2002**, *59*, 438−449.
(12) Mao, J.; Zhao, L.; Yao, K.; Shang, Q.; Yang, G.; Cao, Y. *J. Biomed. Mater. Res. A* **2003**, *64A*, 301−308.
(13) Gingras, M.; Paradis, I.; Berthod, F. *Biomaterials* **2003**, *24*, 1653−1661.
(14) Ma, L.; Shi, Y.; Chen, Y.; Zhao, H.; Gao, C.; Han, C. *J. Mater. Sci. Mater. Med.* **2007**, *18*, 2185−2191.
(15) Suwan, J.; Zhang, Z.; Li, B.; Vongchan, P.; Meepowpan, P.; Zhang, F.; Mousa, S.; Premanode, B.; Kongtawelert, P.; Linhardt, R. *Carbohydr. Res.* **2009**, *344*, 1190−1196.
(16) Lin, W.-C.; Liu, T.-Y.; Yang, M.-C. *Biomaterials* **2004**, *25*, 1947−1957.
(17) Richert, L.; Lavalle, P.; Payan, E.; Shu, X. Z.; Prestwich, G. D.; Stoltz, J. F.; Schaaf, P.; Voegel, J. C.; Picart, C. *Langmuir* **2004**, *20*, 448−458.
(18) Decher, G.; Lehr, B.; Lowack, K.; Lvov, Y.; Schmitt, J. *Biosens. Bioelectron.* **1994**, *9*, 677−684.
(19) Decher, G.; Eckle, M.; Schmitt, J.; Struth, B. *Curr. Opin. Colloid Interface Sci.* **1998**, *3*, 32−39.
(20) Lvov, Y. M.; Decher, G. *Kristallografiya* **1994**, *39*, 696−716.
(21) Shiratori, S. S.; Rubner, M. F. *Macromolecules* **2000**, *33*, 4213−4219.
(22) Sui, Z. J.; Salloum, D.; Schlenoff, J. B. *Langmuir* **2003**, *19*, 2491−2495.
(23) Tan, H. L.; McMurdo, M. J.; Pan, G. Q.; Van Patten, P. G. *Langmuir* **2003**, *19*, 9311−9314.
(24) Bravo, J.; Zhai, L.; Wu, Z.; Cohen, R. E.; Rubner, M. F. *Langmuir* **2007**, *23*, 7293−7298.
(25) Jisr, R.; Rmaile, H.; Schlenoff, J. B. *Angew. Chem., Int. Ed.* **2004**, *44*, 782−785.
(26) Wood, K. C.; Boedicker, J. Q.; Lynn, D. M.; Hammond, P. T. *Langmuir* **2005**, *21*, 1603−1609.
(27) Yan, Y.; Such, G. K.; Johnston, A. P. R; Lomas, H.; Caruso, F. *ACS Nano* **2011**, *5*, 4252−4257.
(28) Priolo, M.; Gamboa, D.; Holder, K.; Grunlan, J. C. *Nano Lett.* **2010**, *10*, 4970−4974.
(29) Yang, Y.-H.; Haile, M.; Park, Y. T.; Malek, F. A.; Grunlan, J. C. *Macromolecules* **2011**, *44*, 1450−1459.
(30) Wu, B. Y.; Hou, S. H.; Yu, M.; Qin, X.; Li, S.; Chen, Q. *Mater. Sci. Eng., C* **2009**, *29*, 346−349.
(31) Gao, Q. A.; Guo, Y. Y.; Zhang, W. Y.; Qi, H. L.; Zhang, C. X. *Sens. Actuators, B* **2011**, *153*, 219−225.
(32) Salimi, A.; Noorbakhsh, A. *Electrochim. Acta* **2011**, *56*, 6097−6105.
(33) Dvoracek, C. M.; Sukhonosova, G.; Benedik, M. J.; Grunlan, J. C. *Langmuir* **2009**, *25*, 10322−10328.
(34) Podsiadlo, P.; Paternel, S.; Rouillard, J. M.; Zhang, Z. F.; Lee, J.; Lee, J. W.; Gulari, L.; Kotov, N. A. *Langmuir* **2005**, *21*, 11915−11921.
(35) Lichter, J. A.; Van Vliet, K. J.; Rubner, M. F. *Macromolecules* **2009**, *42*, 8573−8586.
(36) Li, Y. C.; Schulz, J.; Mannen, S.; Delhom, C.; Condon, B.; Chang, S.; Zammarano, M.; Grunlan, J. C. *ACS Nano* **2010**, *4*, 3325−3337.
(37) Laufer, G.; Carosio, F.; Martinez, R.; Camino, J.; Grunlan, J. C. *J. Colloid Interface Sci.* **2011**, *356*, 69−77.
(38) Li, Y.-C.; Mannen, S.; Morgan, A. B.; Chang, S.; Yang, Y.-H.; Condon, B.; Grunlan, J. C. *Adv. Mater.* **2011**, *23*, 3926−3931.
(39) Podsiadlo, P.; Kaushik, A. K.; Arruda, E. M.; Waas, A. M.; Shim, B. S.; Xu, J.; Nandivada, H.; Pumplin, B. G.; Lahann, J.; Ramamoorthy, A.; Kotov, N. A. *Science* **2007**, *318*, 80−83.
(40) Podsiadlo, P.; Tang, Z.; Shim, B. S.; Kotov, N. A. *Nano Lett.* **2007**, *7*, 1224−1231.
(41) Kim, D. W.; Kumar, J.; Blumstein, A. *Appl. Clay Sci.* **2005**, *30*, 134−140.

(42) Li, Y.-C.; Schulz, J.; Grunlan, J. C. *ACS Appl. Mater. Interfaces* **2009**, *1*, 2338−2347.
(43) Priolo, M.; Gamboa, D.; Grunlan, J. C. *ACS Appl. Mater. Interfaces* **2010**, *2*, 312.
(44) Hickey, J.; Burke, N. A. D.; Stöver, H. D. H. *J. Membr. Sci.* **2011**, *369*, 68−76.
(45) Yang, Y.-H.; Malek, F. A.; Grunlan, J. C. *Ind. Eng. Chem. Res.* **2010**, *49*, 8501−8509.
(46) Ray, S. S.; Okamoto, M. *Prog. Polym. Sci.* **2003**, *28*, 1539−1641.
(47) Hirschler, M. M. *Polym. Adv. Technol.* **2008**, *19*, 521−529.
(48) Jarerat, A.; Tokiwa, Y. *Macromol. Biosci.* **2001**, *1*, 136−140.
(49) Garlotta, D. *J. Polym. Environ.* **2001**, *9*, 63−84.
(50) Auras, R.; Harte, B.; Selke, S. *J. Appl. Polym. Sci.* **2004**, *92*, 1790−1803.
(51) Simchi, A.; Pishbin, F.; Boccaccini, A. R. *Mater. Lett.* **2009**, *63*, 2253−2256.
(52) Drumright, R. E.; Gruber, P. R.; Henton, D. E. *Adv. Mater.* **2000**, *12*, 1841−1846.
(53) Plackett, D. V.; Holm, V. K.; Johansen, P.; Ndoni, S.; Nielsen, P. V.; Sipilainen-Malm, T.; Sodergard, A.; Verstichel, S. *Packag. Technol. Sci.* **2006**, *19*, 1−24.
(54) Jin, T.; Zhang, H. *J. Food Sci.* **2008**, *73*, M127−M134.
(55) Auras, R.; Singh, S. P.; Singh, J. J. *Packag. Technol. Sci.* **2005**, *18*, 207−216.
(56) Cussler, E. L.; Hughes, S. E.; Ward, W. J. III; Arias, R. *J. Membr. Sci* **1988**, *38*, 161−174.
(57) Duncan, T. V. *J. Colloid Interface Sci.* **2011**, *363*, 1−24.
(58) Roberts, A. P.; Henry, B. M.; Sutton, A. P.; Grovenor, C. R. M.; Briggs, G. A. D.; Miyamoto, T.; Kano, A.; Tsukahara, Y.; Yanaka, M. *J. Membr. Sci.* **2002**, *208*, 75−88.
(59) Butler, B. L.; Vergano, P. J.; Testin, R. F.; Bunn, J. M.; Wiles, J. L.
J. Food Sci. **1996**, *61*, 953−956.
(60) Caner, C.; Vergano, P. J.; Wiles, J. L. *J. Food Sci.* **1998**, *63*, 1049−1053.
(61) Oguzlu, H.; Tihminlioglu, F. *Macromol. Symp.* **2010**, *298*, 91−98.
(62) Chang, J.-H.; An, Y. U.; Sur, G. S. *J. Polym. Sci., Part B: Polym. Phys.* **2003**, *41*, 94−103.
(63) Lange, J.; Wyser, Y. *Packag. Technol. Sci.* **2003**, *16*, 149−158.
(64) Kramer, R. H.; Zammarano, M.; Linteris, G. T.; Gedde, U. W.; Gilman, J. W. *Polym. Degrad. Stab.* **2010**, *95*, 1115−1122.
(65) Schartel, B.; Hull, T. R. *Fire Mater.* **2007**, *31*, 327−354.
(66) Zhao, C.; Qin, H.; Gong, F.; Feng, M.; Zhang, S.; Yang, M. *Polym. Degrad. Stab.* **2005**, *87*, 183−189.
(67) Morgan, A. B.; Chu, L.-L.; Harris, J. D. *Fire Mater.* **2005**, *29*, 213−229.
(68) Qin, H.; Zhang, S.; Zhao, C.; Hu, G.; Yang, M. *Polymer* **2005**, *46*, 8386−8395.
(69) Dasari, A.; Yu, Z.-Z.; Mai, Y.-W.; Cai, G.; Song, H. *Polymer* **2009**, *50*, 1577−1587.
(70) Annabi-Bergaya, F. *Microporous Mesoporous Mater.* **2008**, *107*, 141−148.
(71) Ploehn, H. J.; Liu, C. Y. *Ind. Eng. Chem. Res.* **2006**, *45*, 7025−7034.